AEROTHERMAL ENVIRONMENT METHODOLOGY OF THE HEXAFLY-INT EXPERIMENTAL FLIGHT TEST VEHICLE (EFTV)

Giuseppe Pezzella [(1)], Valerio Carandente [(2)], Roberto Scigliano [(3)], Marco Marini [(4)], Johan Steelant [(5)]

[(1)] *Italian Aerospace Research Centre (CIRA), Via Maiorise snc, 81043 Capua, Italy, Email: g.pezzella@cira.it*
[(2)] *Italian Aerospace Research Centre (CIRA), Via Maiorise snc, 81043 Capua, Italy, Email: v.carandente@cira.it*
[(3)] *Italian Aerospace Research Centre (CIRA), Via Maiorise snc, 81043 Capua, Italy, Email: r.scigliano@cira.it*
[(4)] *Italian Aerospace Research Centre (CIRA), Via Maiorise snc, 81043 Capua, Italy, Email: m.marini@cira.it*
[(5)] *European Space Agency (ESA), Keplerlaan 1, 2201 AZ Noordwijk, Netherlands, Email: johan.steelant@esa.int*

ABSTRACT

Over the last years, innovative concepts of civil high-speed transportation vehicles and the development of related technologies were proposed in EC co-funded projects like ATLLAS, LAPCAT and HEXAFLY [1-3]. These vehicles have a strong potential to increase the cruise range efficiency at high Mach numbers, thanks to efficient propulsion units combined with high-lifting vehicle concepts. Nonetheless, performing a flight test will be the only and ultimate proof to demonstrate the technical feasibility of these new promising concepts and technologies and would result into a major breakthrough in high-speed flight.

In this frame the Hexafly-INT project intends to test in free-flight conditions an innovative gliding vehicle with several breakthrough technologies on-board. This approach will create the basis to gradually increase the readiness level of a consistent number of technologies suitable for high-speed flying systems.

This work describes the methodology and the implementation of tools for thermal analysis of the Hexafly-INT Experimental Flight Test Vehicle, namely EFTV, during a preliminarily considered test window. The paper will present the environment during the test window at cruise Mach numbers, in particular regarding aerothermodynamic loads acting on the vehicle along the flight path. Then, preliminary results of a Finite Element thermal analysis, useful to perform a proper material selection, will be presented and discussed.

1. INTRODUCTION

Over the last years, innovative concepts of civil high-speed transportation vehicles were proposed. These vehicles have a strong potential to increase the cruise range efficiency at high Mach numbers, thanks to efficient propulsion units (turbojets based on air-turbo-rocket cycle for take-off and landing, and dual-mode ramjet/scramjet for cruise) combined with high-lifting vehicle concepts [4,5].

Nonetheless, performing a flight test will be the only and ultimate proof to demonstrate the technical feasibility of these new promising concepts and would result into a major breakthrough in high-speed flight. At present, the expected performances are usually demonstrated by numerical simulations and partly experimentally. As high-speed wind tunnels are intrinsically limited in size or test duration, it is nearly impossible to fit even modest vehicle plan-form completely into a tunnel. Therefore experiments are limited either to the internal propulsive flow-path with combustion, but without the presence of high-lifting surfaces, or to complete small-scaled aero-models, but without the presence of a combusting propulsion unit. Though numerical simulations are less restrictive in geometrical size, they struggle however with accumulated uncertainties in their modelling, making predictions doubtful without in-flight validation. As a consequence, the obtained technology developments are now limited to a technology readiness level of TRL equal to 4 (components validated in laboratory).

The HEXAFLY-INT project aims at the free flight testing of an innovative high-speed vehicle with several breakthrough technologies on board. This approach will create the basis to gradually increase TRL.

The vehicle design, manufacturing, assembly and verification will be the main driver and challenge in this project, in combination with a mission tuned sounding rocket. The prime objectives of this free-flying high-speed cruise vehicle shall aim at [4]:

- a conceptual design demonstrating a high aerodynamic efficiency at cruise with a high volumetric efficiency;
- a positive aerodynamic balance at a controlled cruise Mach numbers from 7 to 8;
- a good gliding performance from Mach 7 to 2;
- an optimal use of advanced high-temperature materials and/or structures.

The main preliminary flight sequence profile and events are shown and listed in Fig. 1 and in Tab. 1, respectively. Then, the EFTV configuration under consideration is depicted in Fig. 2.

In the present work the methodology and the implementation of tools for thermal analysis of the EFTV, during a preliminarily considered test window, is presented. Thermal analyses are performed in the most critical phase of the mission, on the basis of the trajectory provided by Gas Dynamics Limited (GDL). In particular, the calculations show a first feasibility analysis for the preliminarily selected materials.
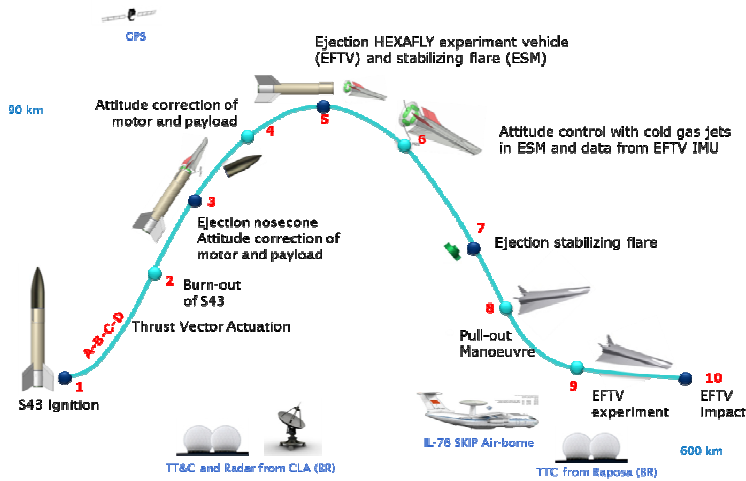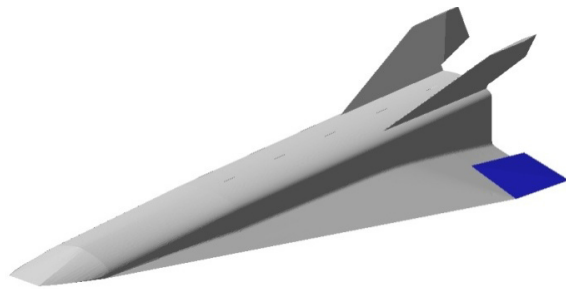
Figure 1. Flight sequence profile [5]

Table 1. Flight sequence events [5]

#	Flight Event
1-2	Propelled ascent
2	Motor burnout
3	Nose-cone ejection
4	L/V alignment
5	ESM/EFTV release
6	Attitude control by RCS in the ESM
7	Ejection of ESM
8	Pull-out manoeuvre
9	Controlled flight
10	Impact

Figure 2. Analyzed vehicle configuration

2. FLIGHT TRAJECTORY

Flight Mechanics analysis developed so far refers to different trajectories provided by GDL. They correspond to different payload masses and altitudes release of the experimental vehicle (EFTV) docked with the support module (ESM). For instance, Fig. 3 shows the trajectory obtained for a payload mass of 400 kg released by the launcher at 90 km altitude (i.e., trajectory apogee).
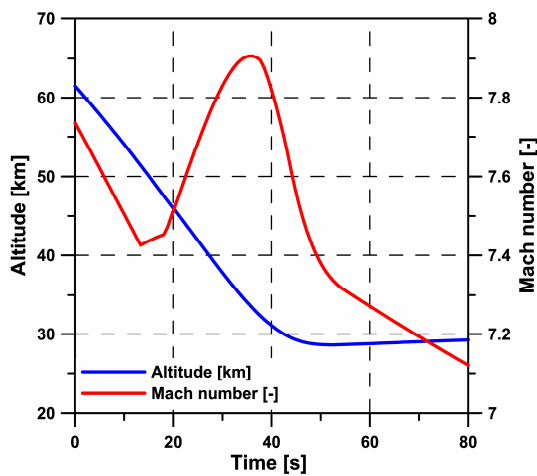

Figure 3. Altitude and Mach number profiles for the preliminarily considered test window of EFTV vehicle

In particular, Fig. 3 provides the time histories of altitude and Mach number profiles during descent starting from 60 km altitude. This preliminary trajectory results in the most conservative scenario in terms of aero-thermal and mechanical loads available so far. Indeed, the profile of the stagnation point convective heat transfer coefficient, provided as input to the thermal analysis hereinafter discussed, is shown in Fig. 4.
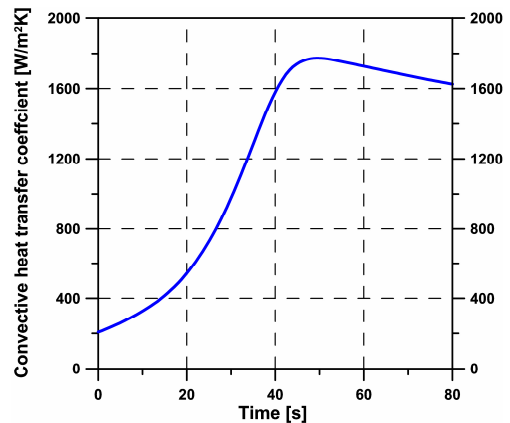

Figure 4. Stagnation point convective heat transfer coefficient estimated along the preliminarily considered test window of EFTV vehicle by means of Tauber's formula

This coefficient was obtained according to the Tauber [6] relationship for the estimation of the convective heat flux at vehicle stagnation point throughout the descent shown in Fig. 3.

A preliminary assessment of laminar-to-turbulent transition has been also performed. Boundary layer transition is usually based on local flow conditions such as local Mach and Reynolds numbers. However, because the assessment of the local flow condition demands accurate CFD computations which are, of course, out of the present design effort, a transition method based on free-stream Reynolds (Re_∞) and Mach numbers (M_∞) has been adopted, according to Eq. (1).

As in [7], the transitional Reynolds limit reads:

$$Log\mathrm{Re}_\infty > \left[Log\mathrm{Re}_T + C_m(M_\infty) \right] \qquad (1)$$

where Re_T and C_m depend on the type of flow, angle of attack, leading edge sweep angle, and leading edge nose bluntness. According to this transition criterion, below 35 km altitude turbulent flow conditions are expected for the EFTV. As a result, at the peak heating condition derived in Fig. 4, attained at $H_\infty=32$ km, $M_\infty=7.88$, $p_\infty=889.1$ Pa and $T_\infty=228$ K, the flowfield past the vehicle is expected to be in turbulent conditions.

3. AEROTHERMODYNAMIC CALCULATIONS

A CFD calculation in turbulent flow conditions is carried out at the trajectory peak heating in order to provide the convective heat flux normalized surface distribution for the subsequent thermal analyses.

Numerical analysis of the flowfield past the EFTV was performed on a hybrid mesh. The overall number of cells is about 5-million (for half body). The distribution of surface grid points was dictated by the level of resolution desired in various areas of vehicle such as stagnation region and base fillet, according to the computational goals and requirements. Grid refinement in regions of flowfield characterized by strong gradients was made through a solution adaptive approach. Indeed, an iterative shock-fitting procedure is carried out in order to properly accommodate the bow shock shape. The air is modelled as an ideal gas. Indeed, the ideal gas assumption can be considered still valid in this case, considering that the Mach number here considered is less than 8. In addition, the EFTV aeroshape features a very slender configuration (leading edge radius of 2 mm) that shall fly at rather low angle of attack (i.e. behind a weak attached bow shock). CFD results for pressure and heat flux normalized surface distributions are provided in Fig. 5 and Fig. 6, respectively.

Surface pressure and heat flux contours point out that the vehicle nose and leading edges are the most solicited
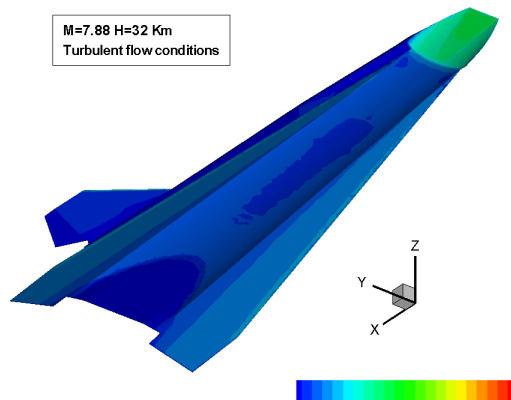

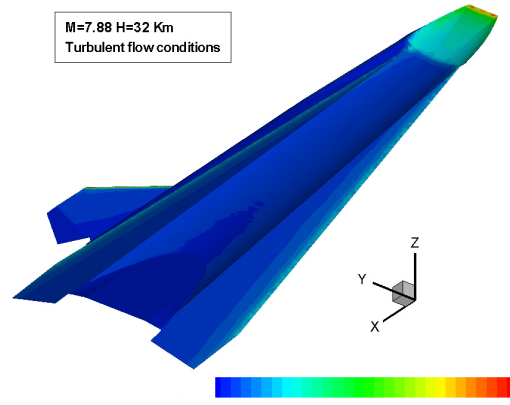*Figure 5. Pressure contour in the maximum heat flux condition (H=32 km, M=7.88)*

Figure 6. Convective heat flux contour in the maximum heat flux condition (H=32 km, M=7.88)

vehicle parts, while on the remaining aeroshape a quite smooth evolution of loading conditions is expected.

4. EFTV CANDIDATE MATERIALS

Different classes of materials have been preliminarily selected and analysed for the EFTV structure, namely: titanium alloy, copper, C/C-SiC and zirconia for surface coatings. This should give a first estimate of the characteristic behaviour of potential materials specifically for this flight trajectory.

Titanium alloys exhibit a unique combination of mechanical and physical properties and corrosion resistance which have made them desirable for critical, demanding aerospace applications, also in high temperatures conditions. Copper is employed as a heat sink to accommodate the thermal energy in some critical components (e.g. nose, leading edges) [8]. C/C-SiC developed at DLR and tested in different high temperatures applications (e.g. HIFiRE and SHEFEX) is considered for ailerons and for a part of the wing leading edge [9]. A zirconia coating layer has been also considered to protect titanium and copper components, increasing the surface emissivity and confining the larger temperatures on the layer itself.

Thermal and mechanical properties of titanium alloy and zirconia coating have been provided by TsAGI, Tsentralniy Aerogidrodinamicheskiy Institut (Central Aerohydrodynamic Institute), which is in charge of the system manufacturing.

In particular, the following assumptions, reported in Tab. 2, have been carried out on the vehicle components shown in Fig. 7 to assess the correct implementation of the methodology:

- copper for the vehicle nose;
- copper for the fore and the aft part of the wing leading edges;
- C/C-SiC for the central part of the wing leading edge;
- copper for the leading edge of the v-tails;
- C/C-SiC for the ailerons;
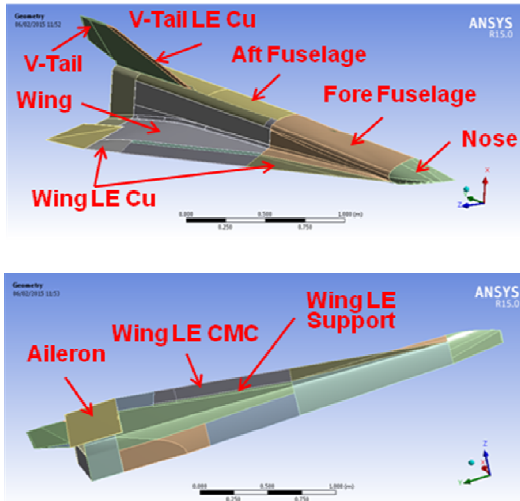- titanium alloy for the remaining part of the structure.

Figure 7. Main structural components of the analysed EFTV

Table 2.Preliminarily material assignment for the main structural components

Nose	Fuselage	Wing
Copper	Ti-Alloy	Ti-Alloy
Wing LE	**V-Tail**	**Aileron**
C/C-SiC / Copper	Ti-Alloy / Copper	C/C-SiC

In addition, as previously mentioned, a layer of 1 mm thick zirconia has been foreseen for all the components in titanium alloy and copper. Using a conservative approach, a constant surface emissivity of 0.4 has been set for the external coated surfaces.

5. THERMAL ANALYSIS

5.1 Numerical procedure

The vehicle thermal behaviour has been preliminary assessed by means of the Finite Element method implemented in the software Ansys [10-11]. A transient analysis along the computed entry path is performed to evaluate the time dependent temperature of the structure. In synthesis, as also schematically reported in Fig. 8, the following procedure has been carried out:

- the available CAD drawing of the vehicle is implemented in Ansys Workbench and properly modified, if required;
- the computational mesh for the subsequent analyses is generated;
- the transient thermal analysis is set assuming as boundary condition the convective heat flux spatial distribution, normalized with respect to the corresponding value, as reported in Fig. 6. This distribution is step by step scaled by the convective heat transfer coefficient variation along the trajectory (see Fig. 4). A radiative dissipation condition is also considered for all the external surfaces;
- static structural computations can be then carried out, if required, in the most critical conditions along the trajectory, assigning as boundary conditions the temperature distributions previously evaluated at selected instants along the trajectory and the pressure distribution resulting from CFD analyses.
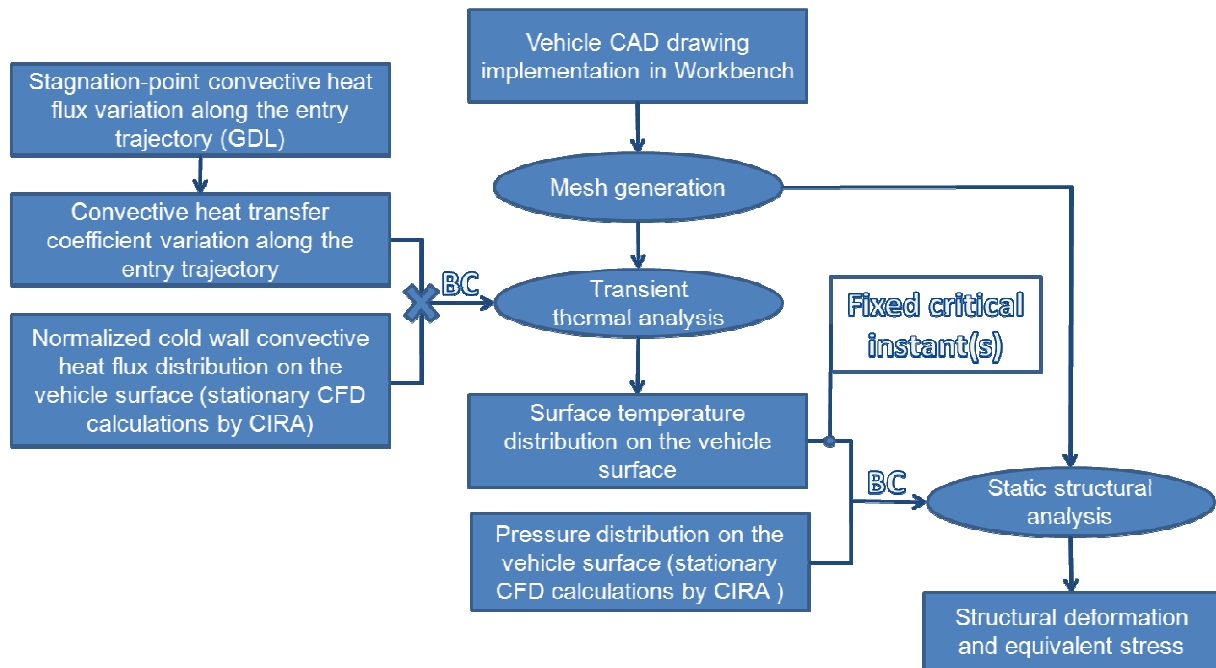

Figure 8. Numerical procedure flow chart

It is now worth underlining that, as previously mentioned, the heat flux boundary conditions for the transient thermal analysis has been assigned in terms of the convective heat transfer coefficient, so that the numerical code can take into account the effective heat flux entering the structure as the wall temperature increases under the heating process (see Eq. 2). Eq. 2 also assumes an ideal gas with constant specific heat.

$$\dot{q} = h \cdot (T_0 - T_w) \approx \frac{\dot{q}_{cw}}{T_0} \cdot (T_0 - T_w) =$$
$$= \frac{\dot{q}_{hw}}{T_0 - T_{w,eq}} \cdot (T_0 - T_w) \tag{2}$$

It is clear that also the convective heat transfer coefficient at any point of the vehicle surface and at a certain time instant is assigned multiplying the value at that time (resulting from the corresponding heat flux value according to Eq. 2), by the normalized convective heat flux derived from CFD calculations. This procedure therefore assumes that the non-dimensional convective heat flux distribution on the vehicle surface is unvaried along the trajectory.

5.2   Preliminary results

As results, according to the previously discussed method, the temporal variation of the maximum temperature on the different analysed materials and vehicle components has been plotted along the flight path. Fig. 9 and Fig. 10 report in particular the maximum temperature variation along the flight profile for different areas of the zirconia coating and for the main vehicle components, respectively.
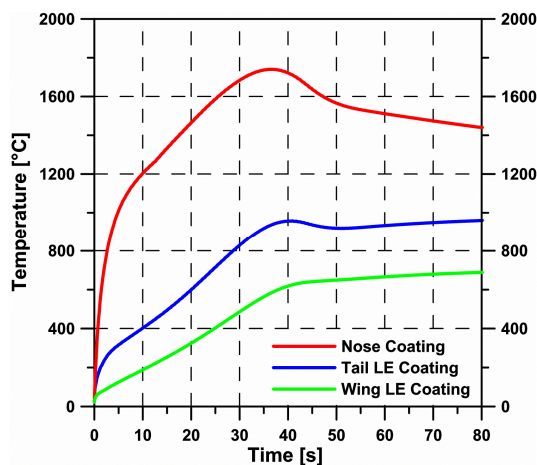

Figure 9. Maximum temperature profiles on zirconia coatings

From Fig. 9 it can be seen that zirconia coatings would widely survive the aerothermal environment in these conditions. From Fig.10 it can be noted that also copper and C/C-SiC would survive in this preliminarily defined

test window. On the other hand, the maximum temperature on the titanium structure exceeds 600°C, usually defined as its upper working temperature limit, but only in limited spots of the vehicle, coloured in red in Fig. 11.
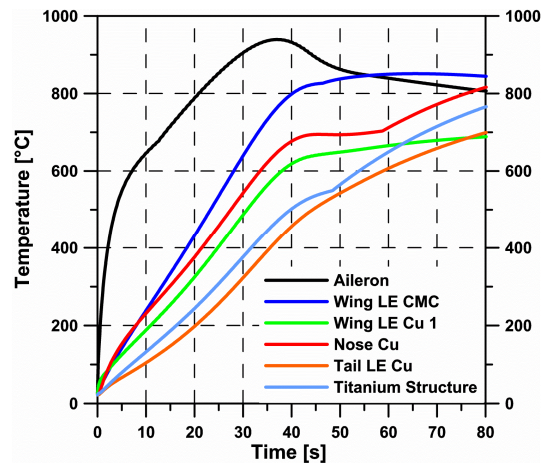

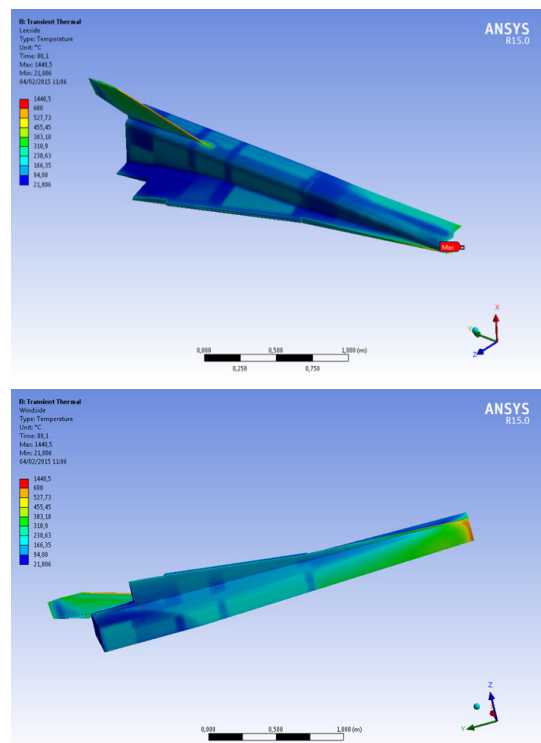Figure 10. Maximum temperature profiles on the main vehicle components

Figure 11. Temperature distribution, at the final time step, on the titanium structure, on the vehicle leeside and windside

6.   CONCLUSIONS

Finally, it can be concluded that:
- a thermal model has been realized for the entire structure on the basis of aerothermal loads estimated along the flight path;

- zirconia coating guarantees a relatively large surface emissivity and a suitable thermal protection for the underlying materials;
- titanium structure can withstand the aerothermal environment except for limited spots, requiring a proper thermal structural optimization;
- copper seems to be adequate for leading edges, considering its ability to work as a heat sink;
- thermal structural design is still ongoing and a numerical analysis campaign will be perform on updated structural configuration, flight trajectory and aerothermal environment.

7. ACKNOWLEDGMENT

8. REFERENCES

1. Steelant J. (2009). Achievements obtained on Aero-Thermal Loaded Materials for High-Speed Atmospheric Vehicles within ATLLAS. In Proc. 16th AIAA/DLR/DGLR "International Space Planes and Hypersonic Systems and Technologies Conference", Bremen, Germany, AIAA-2009-7225.

2. Steelant, J. (2011). Sustained Hypersonic Flight in Europe: first achievements within LAPCAT II. In Proc. 17th AIAA "International Space Planes and Hypersonic Systems and technologies conference", San Francisco, California, AIAA 2011-2243.

3. Steelant, J. et al. (2015). Conceptual Design of the High-Speed Propelled Experimental Flight Test Vehicle HEXAFLY. In Proc. 20th AIAA "International Space Planes and Hypersonic Systems and technologies conference", Glasgow, Scotland.

4. Hexafly-INT Team (2014). Part B "High-Speed Experimental Fly Vehicles–INTernational", CIRA-CF-14-1132

5. Jung, W., Ettl, J., Kallenbach, A., Turner, J. (2014). Mission Definition and System Requirements, Work Package 2.0 – Launch Vehicle, Presentation at HEXAFLY-INT MDR & SRR, Capua, Italy

6. Tauber, M.E. (1989). A review of high-speed, convective, heat-transfer computation methods. Technical Paper 2914, NASA.

7. Quinn, R.D., Gong, L. (1990). Real-Time Aerodynamic Heating and Surface Temperature Calculations for Hypersonic Flight Simulation. Technical Memorandum 42522, NASA.

8. Weast, R.C. (1999). *CRC Handbook of Chemistry and Physics*, CRC Press, Boca Raton, FL, 80th Edition

9. Glass, D.E., Capriotti, D.P., Reimer, T., Kütemeyer, M., Smart, M. (2014). Testing of DLR C/C-SiC and C/C for HIFiRE 8 Scramjet Combustor. In Proc- 19th AIAA "International Space Planes and Hypersonic Systems and Technologies Conference", Atlanta, Georgia

10. ANSYS Inc. (2009). Thermal analysis guide, Release 12.1.

11. ANSYS Inc. (2009). Structural analysis guide, Release 12.1.